Data Repository

for

Global importance of oxic molybdenum sinks prior to 2.6 Ga revealed by the Mo isotope composition of Precambrian carbonates

1. Mo sources and sinks and isotope systematics in modern environments

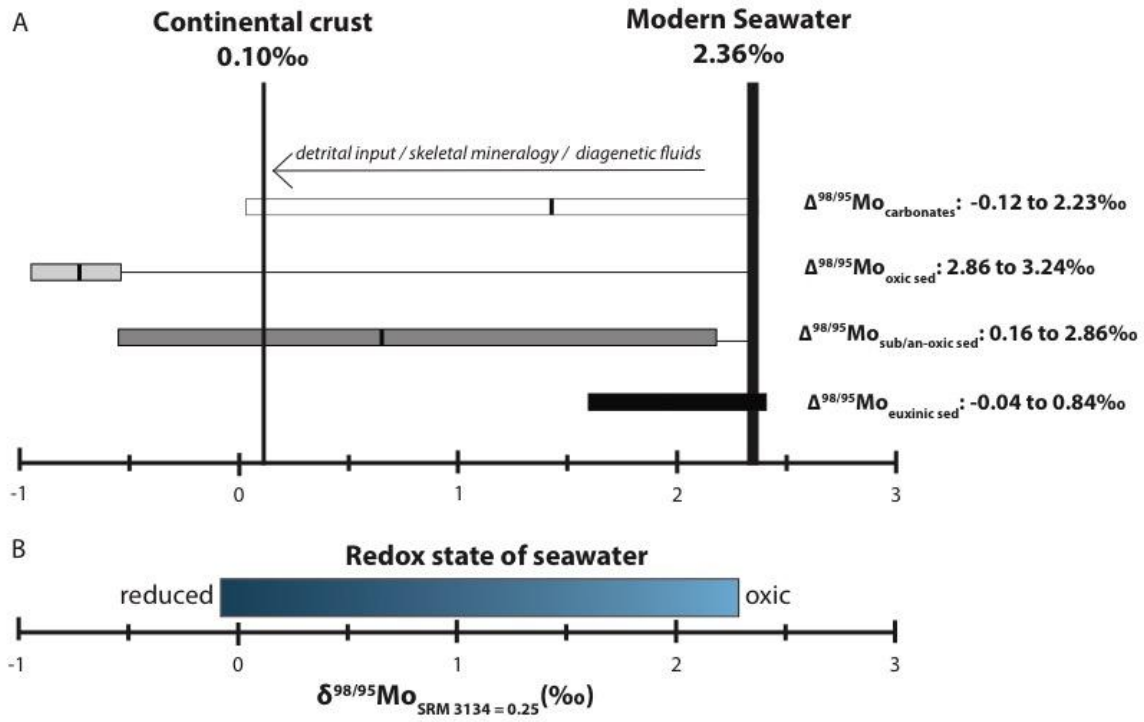

Figure DR1. A: Isotope fractionation of Mo from modern seawater to selected sedimentary Mo archives and major sinks: carbonates (Voegelin et al., 2009); oxic sediments (Barling et al., 2001, Siebert et al., 2003); suboxic and anoxic sediments (Barling et al., 2001, Siebert et al., 2003, Siebert et al., 2006, and Poulson et al., 2006); and euxinic sediments (Barling et al., 2001, Arnold et al., 2004). All Mo isotope compositions have been recalculated as δ^{98}Mo relative to the standard reference material NIST 3134=0.25‰ (Table DR1, Greber et al., 2012, Nägler et al., 2014, Goldberg et al., 2013). B: Oxidation state of seawater relative to its molybdenum isotopic signature.

2. Description of samples and localities

a. <u>Modern microbialitic carbonate samples from the Bahamas</u>

Four modern thrombolites and four modern stromatolites were sampled at Highborne Cay, Northern Exumas, Bahamas in March 2010 (Myshrall et al., 2010). They formed in modern oxic seawater with a temperature of 25°C and a salinity of 33-35.5 PSU (Edgcomb et al.,

2014). These cm-to-m-scale microbialites contain microbial mats with cyanobacteria, and some mollusks are present (Myshrall et al., 2010). O_2 and sulfide measurements on similar stromatolitic and thrombolitic samples revealed an oxic first centimeter with anoxic sediments below (Myshrall et al., 2010; Edgcomb et al., 2014).

b. 2.52 Ga stromatolitic carbonates, Gamohaan Formation, Campbellrand Subgroup

Outcrop samples of stromatolitic carbonates from the Gamohaan Formation, in the upper part of the Campbellrand Subgroup (Ghaap Group, Transvaal Supergroup, South Africa; from locations 27°23.000'S, 23°20.833'E and 27°37.666'S, 23°24,050'E), were provided by Dawn Sumner. The Gamohaan Formation is dated at 2.52 Ga (Sumner and Bowring, 1996) and 2.516 Ga (Altermann and Nelson, 1998) by U-Pb dating of zircon from volcanic ash beds. The sedimentology of the Gamohaan Formation was detailed by Sumner, (1997), and Sumner and Grotzinger, (2004). Variability in the nature of microbialitic carbonates is significant (Sumner, 1997), ranging from cm-scale planar and contorted laminar mat assemblages to decimeter-scale columnar and bedded cuspate assemblages. The sedimentology near stromatolites indicates a deep subtidal and sub-wave-base depositional environment (Sumner and Grotzinger, 2004). Previous REE data from Gamohaan carbonates have shown an important hydrothermal input (strong Eu anomaly and primitive Nd isotope composition; Kamber and Webb, 2001). Moreover, the REE patterns indicate the precipitation of these carbonates from shallow water in an open anoxic basin (Kamber et al., 2014).

c. 2.80 Ga microbialitic carbonates and crystal fans, Mosher Carbonate, Wabigoon Subprovince

The Mosher Carbonate is part of the Steep Rock Group in the Wabigoon Subprovince of the Canadian Shield (48°47.717'N, 91°38.000'W and 48°48.983'N, 91°38,367'W). It was age-constrained to older than 2780 Ma by U-Pb dating of zircon from the overlying komatiite

(Tomlinson et al., 2003; Fralick et al., 2008) with underlying sandstone providing a detrital zircon age of less than 2801 Ma (youngest zircon 2779±22 Ma, Denver Stone, personal communication). Previous sedimentological studies have demonstrated excellent preservation of biogenic and abiotic features (microbialites, digital stromatolites, crystal fans) in the Mosher carbonate (Veizer et al., 1982). The carbonate was deposited as the ocean transgressed over bedrock channels cut into the top of a mafic volcanic dominated ocean plateau (Fralick et al., 2008). Carbonate production was able to keep pace with relative rise of sea-level until, after deposition of 200 to 500 meter of carbonate, deepening water caused iron formation to laterally move over the platform. This platform has been identified as an oxygen oasis within an otherwise anoxic ocean (Riding et al., 2014; Fralick and Riding, 2015). Microbialite and stromatolite samples (P-09 and P-10) come from the central lagoonal area, while crystal fan samples (P-02 and P-06) come from giant domes that formed the outer raised edge of the platform, semi-isolating it from the ocean (Wilks and Nisbet, 1984; Riding et al., 2014; Fralick and Riding, 2015). All samples were obtained from outcrop.

d. 2.93 Ga stromatolitic carbonates, Ball Assemblage, Red Lake Greenstone Belt

The Ball assemblage is part of the Red Lake Greenstone Belt in the Uchi Subprovince, Canadian Shield (51°03.000'N, 94°07.017'W and 51°01.867'N, 94°11,400'W). It is dated to between 2.92 and 2.94 Ga by U-Pb dating of zircons (Corfu and Wallace, 1986). The Ball assemblage is dominantly composed of mafic volcanic rocks and their intrusive equivalents, with some accessory stromatolitic carbonates (Corfu and Wallace, 1985; Corfu and Stone, 1998; Sanborn-Barrie et al., 2001). The chemistry of its magmatic rocks reveals a volcanic arc origin with possible plume activity (Sanborn-Barrie et al., 2001). The carbonate formation has been described as a platform with stromatolites, crystal fans, laminated carbonates, carbonate-associated iron formations (IF), and cherts (McIntyre and Fralick, 2017). Previous REE

measurements and sedimentological observations have shown that the carbonates precipitated in a relatively flat-topped shallow-water platform while the IF originated offshore, but in less than 200 meters of water. However, minor regressions could cause semi-restricted and evaporatic conditions, provoking a water density difference and down-welling. Decimeter-scale stromatolites, crystal fans, carbonate crusts, and probable gypsum, now pseudomorph, were deposited on extensive tidal flats, whereas offshore mounds of crystal fans and microbialite dominated landward of the transition to cherts, carbonaceous shales, and iron formation (McIntyre and Fralick, 2017). Recent studies suggest that deposition of the marine carbonate platform occurred during a volcanic hiatus (Sanborn-Barrie et al., 2001; McIntyre and Fralick, 2017). All samples were obtained from decimeter-scale stromatolites sampled in outcrop.

e. 2.97 Ga stromatolitic carbonates, Chobeni Formation, Nsuze Group, Pongola Supergroup

The Chobeni Formation is the middle formation of the Nsuze Group in the White Mfolozi inlier of the Pongola supergroup, South Africa (28°14.476'S, 31°10.313'E and 28°14.437'S, 31°10,300'E). It is dated at 2.97 Ga by U-Pb dating of zircon (Mukasa et al., 2013). Several sedimentary and geochemical studies have assigned the White Mfolozi section deposits to a depositional environment characterized by a tidal channel with intertidal to shallow subtidal influences (Beukes and Lowe, 1989; Siahi et al., 2016; 2018). Samples come from the main carbonate of Chobeni Formation. Half of the samples (1A to 3B) are stromatolitic dolomite obtained from m-scale stromatolitic bioherms, while the remaining samples (8 to 10B) are bedded dolarenites. All samples were obtained from outcrop.

3. Mo isotope measurements

All material used for Mo analysis, from crushing to the isotope measurement, was Mo-free. The Mo purification protocol used is derived from Siebert et al., (2001); Voegelin et al., (2009); and Asael et al., (2013). 1.5 g of powder was digested by 6N HCl; this represents a more rigorous digestion than was performed for trace elements (see section DR5b), dissolving carbonate but also Fe and Mn oxides, as well as likely some clays if present, but leaving more crystalline silicates and recalcitrant minerals intact. This particular digestion protocol was chosen principally for our data to remain comparable to the majority of Mo-carbonate isotope studies that have used this same method (Voegelin et al., 2009; 2010; Eroglu et al., 2015). A ^{97}Mo-^{100}Mo double-spike (DS) was added before digestion. The DS is useful for tracing any isotopic fractionation during chemistry and to correct for instrumental mass bias during the isotope analyses. In order to avoid bias in the measurement and the double spike data reduction, a DS/Natural Mo ratio close to 1 was employed. Due to the low Mo concentration in our samples, Mo was not detected by ThermoFisher Scientific Element2 HR-ICP-MS measurement. Thus, we first tested the sample by the blind addition of DS in order to obtain a first DS/Nat ratio before determining the dose of DS required for making the final sample measurement.

Samples underwent two Mo purification steps. During the first step, samples were Mo- and Fe-purified by anion exchange chromatography on columns filled with Biorad AG1-X8 resin, 200-400 mesh. After adding the sample in 6N HCl solution to the column, the matrix was washed away with 6N HCl and the Fe-Mo fraction eluted with 3N HNO_3. The Mo-Fe cut was dried and the sample taken up in 0.24N HCl to prepare for the second Mo purification step. Subsequently, the Mo was eluted using 0.24 N HNO_3 on a cation exchange column with Biorad AG 50W-X8 resin, 200-400 mesh, while the Fe was eluted to waste using 6N HCl. The pure Mo solution was dried and taken up in 2% HNO_3 for measurement by

ThermoFisher Scientific Neptune MC-ICP-MS (Pôle Spectrometry Océan, Brest, France). The double spike deconvolution method of Siebert et al., (2001) was used to obtain δ^{98}Mo and Mo concentration. Our in-house standard, Mo-SPEX, demonstrated a 2SD reproducibility of 0.09 ‰ across all sessions. Our total blank was 0.6 ng. Our data were acquired relative to Mo-SPEX and converted relative to Roch-Mo2 and then to SRM 3134 (see Table DR1).

For samples analyzed in this study, major element compositions indicate variable degrees of detrital contamination and silicification of the samples (see Figure DR2). δ^{98}Mo values corrected for detrital input ($\delta^{98}Mo_{auth.}$) are provided in Table DR2 when Ti concentrations are known and Mo concentrations enriched above crustal values relative to Ti ($[Mo_{auth}] > 0$, calculated as per Voegelin et al., 2009). The correction was 0.04‰ on average, and results in $\delta^{98}Mo_{auth.}$ values that are shifted away from crustal-like compositions towards more extreme values, thus to be conservative, only non-corrected data were employed for the figures and discussion.

4. Data compilation and differences between shale and carbonate records

This work presents a compilation of molybdenum isotope compositions of shales and carbonates through geological time. These two lithologies are known to record the Mo isotopic signature of the seawater from which they precipitated, as shown in the Figure DR1 (Siebert et al., 2003; Voegelin et al., 2009). These data can indicate the global redox condition of seawater via the preferential uptake of lighter Mo isotopes by Mn- and Fe- oxides; the stronger a role manganese oxides play in marine Mo cycling the more seawater tends towards a heavier molybdenum isotope signature (Figure DR1). This compilation gathers 730 previously reported δ^{98}Mo data from reduced sediments from 24 articles, 201 carbonate

δ^{98}Mo data from 5 articles, and 85 iron formation δ^{98}Mo data from 6 articles (see Tables DR3 to DR5).

Initial $\delta^{97/95}$Mo data have been corrected to δ^{98}Mo by a simple multiplication of 3/2 (Barling et al., 2001; Arnold et al.; 2004; Wen et al., 2011, see Tables DR3 and DR4). All data are expressed relative to the standard NIST SRM 3134 = 0.25‰ in order to compare all data together and to preserve the modern seawater value of 2.36‰ from Siebert et al., 2003 (see Table DR1 for conversion). No detrital correction was applied to carbonate data from Voegelin et al., (2009), from Eroglu et al., (2015), and from Romaniello et al., (2016), nor for most of the shale data, with the exception of three samples from Neubert et al., (2008).

There are several possibilities for the origin of the discrepancy discussed in main text that is apparent between the two lithologies prior to 2.6 Ga. First, not all samples have necessarily been deposited under fully-marine conditions. For instance, some shales in the compiled dataset, specifically those from the 2.76 Ga Hardey Formation and the 2.77 Ga Mount Roe Basalt (Fortescue Group, Wille et al., 2013) are fluvial or lacustrine in origin (Blake, 1993 and Thorne and Trendall, 2001). Furthermore, stromatolitic carbonates and dolarenites from the 2.97 Ga Chobeni Formation appear to have been deposited under brackish water conditions based on sedimentological and Sr isotope data (Siahi et al., 2016; 2018), as well as REE patterns that show some, but not all, features characteristic of seawater (Siahi et al., 2018; this study; Figure 2). However, for the remainder of shales and carbonates older than 2.65 Ga that were compiled or measured for this study, multiple lines of evidence confirm their marine origin (see supplementary discussions on sample provenance and on REE spectra features). Secondly, the localization of the two lithologies at different margin depths, coupled to the heterogeneity of the seawater Mo isotopic signature between shallow and deep waters, may have induced a distinction in the record of seawater composition of shales and carbonates. It is likely that oxidizing niches during the Paleoarchean were localized

to near-shore or lagoonal environments (Lalonde and Konhauser, 2015), such that focused Mn cycling created spatial Mo isotope heterogeneity that was captured by shallow-water carbonate and IF. However, residence times of waters on continental shelves, carbonate platforms, and epeiric seas is generally on the order of days to years, and it is, therefore, difficult to imagine an oceanic Mo residence time smaller than these intervals even at dissolved Mo concentrations that were less than 1000 times modern levels. Such spatial heterogeneity may be possible in highly restricted basins or under conditions of extreme Mo drawdown, and future studies might specifically target such settings to resolve this issue. Third, is that diagenesis may affect δ^{98}Mo values in carbonates (Voegelin et al., 2009; Eroglu et al., 2015; Romaniello et al., 2016; see supplementary discussion on diagenesis). For modern carbonates that are in contact with sulfidic porewaters during early diagenesis, enrichment in [Mo], as well as a trend to heavier δ^{98}Mo values, is observed and results in carbonate δ^{98}Mo values that approach the seawater value. In older carbonates, relationships between δ^{98}Mo and [Mo] is either non-existent (Voegelin et al., 2010; Wen et al., 2011; Eroglu et al., 2015), or if present, inverse to that of modern samples (Voegelin et al. 2010; this study; Figure DR5a).

Multiple factors other than sulfide-dependant enrichment of seawater Mo may influence carbonate Mo isotope compositions, including the addition of oxide-bound Mo, detrital Mo, and increasing degree of silicification (Figure DR4b). All of these processes tend to drive δ^{98}Mo to crustal values, or even lighter, and cannot explain the heavy enrichments observed in our carbonate dataset. As discussed in the main text, the failure of shales deposited prior to 2.6 Ga to experience authigenic Mo enrichment from seawater, and thus record the Mo isotopic composition of seawater, is the most parsimonious explanation for the contrasting values between shales and carbonates at that time.

a. Data sources for shales

Arnold, G. L., Anbar, A., Barling, J., Lyons, T., 2004, Molybdenum isotope evidence for widespread anoxia in mid-Proterozoic oceans: Science, v. 304, p. 87–90, doi: 10.1126/science.1091785.

Asael, D., Tissot, F. L., Reinhard, C. T., Rouxel, O., Dauphas, N., Lyons, T. W., Ponzevera, E., Liorzou, C., Chéron, S., 2013, Coupled molybdenum, iron and uranium stable isotopes as oceanic paleoredox proxies during the Paleoproterozoic Shunga Event: Chemical Geology, v. 362, p. 193–210, doi: 10.1016/j.chemgeo.2013.08.003.

Barling, J., Arnold, G. L., Anbar, A., 2001, Natural mass-dependent variations in the isoto- pic composition of molybdenum: Earth and Planetary Science Letters, v.193, p. 447–457, doi: 10.1016/S0012-821X(01)00514-3.

Dahl, T. W., Canfield, D. E., Rosing, M. T., Frei, R. E., Gordon, G. W., Knoll, A. H., Anbar, A. D., 2011, Molybdenum evidence for expansive sulfidic water masses in ~750 Ma oceans: Earth and Planetary Science Letters v. 311, p. 264–274, doi: 10.1016/j.epsl.2011.09.016.

Dickson, A. J., Cohen, A. S., Coe, A. L., 2012, Seawater oxygenation during the Paleocene- Eocene thermal maximum: Geology, v. 40, p. 639–642, doi: 10.1130/G32977.1.

Dickson, A. J., Jenkyns, H. C., Porcelli, D., van den Boorn, S., Idiz, E., 2016, Basin-scale controls on the molybdenum-isotope composition of seawater during Oceanic Anoxic Event 2 (Late Cretaceous): Geochimica et Cosmochimica Acta, v. 178, p. 291–306, doi: 10.1016/j.gca.2015.12.036.

Duan, Y., Anbar, A. D., Arnold, G. L., Lyons, T. W., Gordon, G. W., Kendall, B., 2010, Molybdenum isotope evidence for mild environmental oxygenation before the Great Oxidation Event: Geochimica et Cosmochimica Acta, v. 74, p. 6655–6668, doi: 10.1016/j.gca.2010.08.035.

Gordon, G., Lyons, T., Arnold, G. L., Roe, J., Sageman, B., Anbar, A., 2009, When do black shales tell molybdenum isotope tales?: Geology v. 37, p. 535–538, doi: 10.1130/G25186A.1.

Herrmann, A. D., Kendall, B., Algeo, T. J., Gordon, G. W., Wasylenki, L. E., Anbar, A. D., 2012, Anomalous molybdenum isotope trends in upper Pennsylvanian euxinic facies: Significance for use of δ^{98}Mo as a global marine redox proxy: Chemical Geology, v. 324, p. 87–98, doi: 10.1016/j.chemgeo.2012.05.013.

Kendall, B., Gordon, G. W., Poulton, S. W., Anbar, A. D., 2011, Molybdenum isotope constraints on the extent of late Paleoproterozoic ocean euxinia: Earth and Planetary Science Letters, v. 307, p. 450–460, doi: 10.1016/j.epsl.2011.05.019.

Kendall, B., Komiya, T., Lyons, T. W., Bates, S. M., Gordon, G. W., Romaniello, S. J., Jiang, G., Creaser, R. A., Xiao, S., McFadden, K., et al., 2015, Uranium and molybdenum isotope evidence for an episode of widespread ocean oxygenation during the late Ediacaran Period: Geochimica et Cosmochimica Acta v. 156, p. 173–193, doi: 10.1016/j.gca.2015.02.025.

Kurzweil, F., Wille, M., Schoenberg, R., Taubald, H., Van Kranendonk, M. J., 2015, Continuously increasing d98Mo values in Neoarchean black shales and iron formations from the Hamersley Basin: Geochimica et Cosmochimica Acta, v. 164, p. 523–542, doi: 10.1016/j.gca.2015.05.009.

Lehmann, B., Nägler, T. F., Holland, H. D., Wille, M., Mao, J., Pan, J., Ma, D., Dulski, P., 2007, Highly metalliferous carbonaceous shale and Early Cambrian seawater. Geology v. 35, p. 403–406, doi: 10.1130/G23543A.1.

Neubert, N., Nägler, T. F., Böttcher, M. E., 2008, Sulfidity controls molybdenum isotope fractionation into euxinic sediments: Evidence from the modern Black Sea: Geology, v.36, p. 775–778, doi: 10.1130/G24959A.1.

Ossa Ossa, F., Hofmann, A., Wille, M., Spangenberg, J. E., Bekker, A., Poulton, S. W., Eickmann, B., Schoenberg, R., 2018, Aerobic iron and manganese cycling in a redox-stratified Mesoarchean epicontinental sea. Earth and Planetary Science Letters, v. 500, p. 28–40, doi: 10.1016/j.epsl.2018.07.044.

Pearce, C. R., Cohen, A. S., Coe, A. L., Burton, K. W., 2008, Molybdenum isotope evidence for global ocean anoxia coupled with perturbations to the carbon cycle during the Early Jurassic: Geology v. 36, p. 231–234, doi: 10.1130/G24446A.1.

Scheiderich, K., Zerkle, A., Helz, G., Farquhar, J., and Walker, R., 2010, Molybdenum isotope, multiple sulfur isotope, and redox-sensitive element behavior in early Pleistocene Mediterranean sapropels: Chemical Geology, v. 279, p. 134–144, doi: 10.1016/j.chemgeo.2010.10.015.

Siebert, C., Nägler, T. F., von Blanckenburg, F., Kramers, J. D., 2003, Molybdenum isotope records as a potential new proxy for paleoceanography: Earth and Planetary Science Letters v. 211, p. 159–171, doi: 10.1016/S0012-821X(03)00189-4.

Siebert, C., Kramers, J., Meisel, T., Morel, P., Nägler, T. F., 2005, PGE, Re-Os, and Mo isotope systematics in Archean and early Proterozoic sedimentary systems as proxies for redox conditions of the early Earth: Geochimica et Cosmochimica Acta, v. 69, p. 1787–1801, doi: 10.1016/j.gca.2004.10.006.

Siebert, C., McManus, J., Bice, A., Poulson, R., Berelson, W. M., 2006, Molybdenum isotope signatures in continental margin marine sediments: Earth and Planetary Science Letters, v. 241, p. 723–733, doi: 10.1016/j.epsl.2005.11.010.

Wille, M., Kramers, J. D., Nägler, T. F., Beukes, N., Schröder, S., Meisel, T., Lacassie, J., Voegelin, A., 2007, Evidence for a gradual rise of oxygen between 2.6 and 2.5 Ga from Mo isotopes and Re-PGE signatures in shales: Geochimica et Cosmochimica Acta, v. 71, p. 2417–2435, doi: 10.1016/j.gca.2007.02.019.

Wille, M., Nebel, O., Van Kranendonk, M. J., Schoenberg, R., Kleinhanns, I. C., Ellwood, M. J., 2013, Mo–Cr isotope evidence for a reducing Archean atmosphere in 3.46–2.76 Ga black shales from the Pilbara, Western Australia: Chemical Geology, v. 340, p. 68–76, doi: 10.1016/j.chemgeo.2012.12.018.

Xu, L., Lehmann, B., Mao, J., Nägler, T. F., Neubert, N., Böttcher, M. E., Escher, P., 2012, Mo isotope and trace element patterns of Lower Cambrian black shales in South China: Multi-proxy constraints on the paleoenvironment: Chemical Geology v. 318, p. 45–59, doi: 10.1016/j.chemgeo.2012.05.016.

Zhou, L., Su, J., Huang, J., Yan, J., Xie, X., Gao, S., Dai, M., et al., 2011, A new paleoen- vironmental index for anoxic events—Mo isotopes in black shales from Upper Yangtze marine sediments: Science China Earth Sciences v. 54, p. 1024–1033, doi: 10.1007/s11430-011-4188-z.

Zhou, L., Wignall, P. B., Su, J., Feng, Q., Xie, S., Zhao, L., Huang, J., 2012, U/Mo ratios and $\delta^{98/95}$Mo as local and global redox proxies during mass extinction events: Chemical Geology v. 324, p. 99–107, doi: 10.1016/j.chemgeo.2012.03.020.

b. Data sources for carbonates

Eroglu, S., Schoenberg, R., Wille, M., Beukes, N., Taubald, H., 2015, Geochemical stratigraphy, sedimentology, and Mo isotope systematics of the ca. 2.58–2.50 Ga-old Transvaal Supergroup carbonate platform, South Africa: Precambrian Research, v. 266, p. 27–46, doi: 10.1016/j.precamres.2015.04.014.

Romaniello, S. J., Herrmann, A. D., Anbar, A. D., 2016, Syndepositional diagenetic control of molybdenum isotope variations in carbonate sediments from the Bahamas: Chemical Geology, v. 438, p. 84–90, doi: 10.1016/j.chemgeo.2016.05.019.

Voegelin, A. R., Nägler, T. F., Samankassou, E., Villa, I. M., 2009, Molybdenum isotopic composition of modern and carboniferous carbonates: Chemical Geology, v. 265, p. 488–498, doi: 10.1016/j.chemgeo.2009.05.015.

Voegelin, A. R., Nägler, T. F., Beukes, N. J., Lacassie, J. P., 2010, Molybdenum isotopes in late Archean carbonate rocks: implications for early Earth oxygenation: Precambrian Research, v. 182, p. 70–82, doi: 10.1016/j.precamres.2010.07.001.

Wen, H., Carignan, J., Zhang, Y., Fan, H., Cloquet, C., Liu, S., 2011, Molybdenum isotopic records across the Precambrian-Cambrian boundary: Geology, v. 39, p. 775–778, doi: 10.1130/G32055.1.

c. Data sources for iron formations

Duan, Y., Anbar, A. D., Arnold, G. L., Lyons, T. W., Gordon, G. W., Kendall, B., 2010, Molybdenum isotope evidence for mild environmental oxygenation before the Great Oxidation Event: Geochimica et Cosmochimica Acta, v. 74, p. 6655–6668, doi: 10.1016/j.gca.2010.08.035.

Kurzweil, F., Wille, M., Schoenberg, R., Taubald, H., Van Kranendonk, M. J., 2015, Continuously increasing d98Mo values in Neoarchean black shales and iron formations from the Hamersley Basin: Geochimica et Cosmochimica Acta, v. 164, p. 523–542, doi: 10.1016/j.gca.2015.05.009.

Kurzweil, F., Wille, M., Gantert, N., Beukes, N. J., Schoenberg, R., 2016, Manganese oxide shuttling in pre-GOE oceans – evidence from molybdenum and iron isotopes: Earth and Planetary Science Letters, v. 452, p. 69-78, doi: 10.1016/j.epsl.2016.07.013.

Planavsky, N., Bekker, A., Rouxel, O. J., Kamber, B., Hofmann, A., Knudsen, A., Lyons, T. W., 2010, Rare earth element and yttrium compositions of Archean and Paleoproterozoic Fe formations revisited: new perspectives on the significance and mechanisms of deposition: Geochimica et Cosmochimica Acta v. 74, p. 6387–6405.

Siebert, C., Kramers, J., Meisel, T., Morel, P., Nägler, T. F., 2005, PGE, Re-Os, and Mo isotope systematics in Archean and early Proterozoic sedimentary systems as proxies for redox conditions of

the early Earth: Geochimica et Cosmochimica Acta, v. 69, p. 1787–1801, doi: 10.1016/j.gca.2004.10.006.

Wille, M., Kramers, J. D., Nägler, T. F., Beukes, N., Schröder, S., Meisel, T., Lacassie, J., Voegelin, A., 2007, Evidence for a gradual rise of oxygen between 2.6 and 2.5 Ga from Mo isotopes and Re-PGE signatures in shales: Geochimica et Cosmochimica Acta, v. 71, p. 2417–2435, doi: 10.1016/j.gca.2007.02.019.

5. Supplemental methods and interpretation

a. Measurement of major elements

An aliquot of each sample powder was digested in 1 ml HNO_3 and 3 ml HF, reacted overnight and neutralized by boric acid before measuring major elements by HORIBA Ultimat2 ICP-AES (Pôle Spectrometry Ocean, Brest, France). Some samples were previously ashed at 500°C to determine the relative loss on ignition (LOI) of the sample (Table DR6). Major element data were employed to constrain detrital contamination, silicification, and the presence of Mn- and Fe-oxides (Figure DR2).

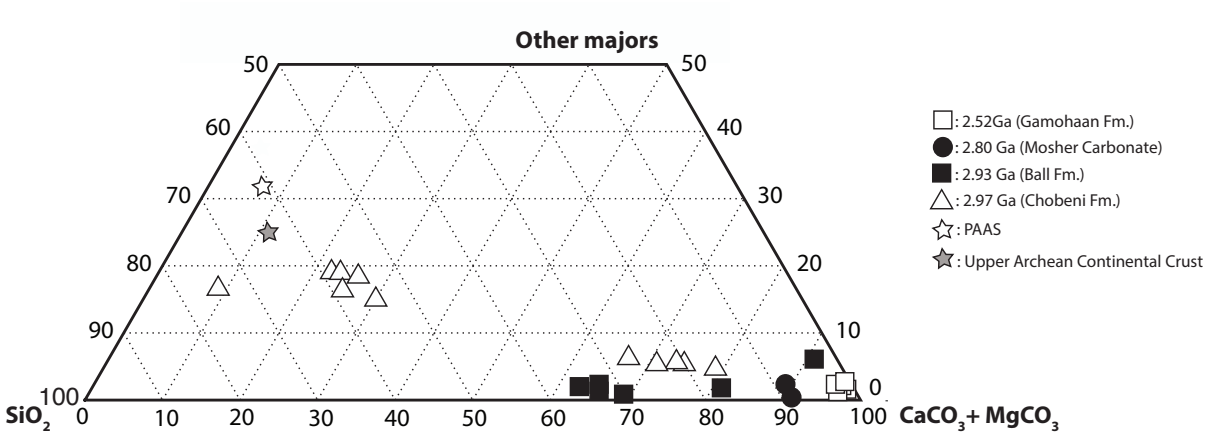

Figure DR2. Ternary diagram representing the degree of purity of carbonate samples ($CaCO_3$+$MgCO_3$; Fe and Mn as $FeCO_3$ and $MnCO_3$ being insignificant at this scale), as well as influences from detrital contamination (TiO_2, Al_2O_3, Fe_2O_3, MnO, Na_2O, K_2O, P_2O_5) and silicification

(SiO_2). Post-Archean Australian Shale (PAAS) and Upper Archean Continental Crust from Taylor & McLennan 1985 are plotted on a CaCO3+MgCO3 scale.

b. REE+Y measurement, normalization, and signatures

An aliquot of each sample powder was digested in 5% trace-metal grade acetic acid according to Rongemaille et al., (2011) in order to extract trace elements from the carbonate phase and evaluate authigenic components derived from seawater without dilution of these signals from detrital material or Fe-Mn oxides that might otherwise dominate the trace element budget at the whole-rock scale. The REE+Y were measured by ThermoFisher Scientific Element2 HR-ICP-MS at the Pôle Spectrometry Océan in Brest, France (Table DR6). REE+Y data for each sample were normalized to the REE+Y composition of Post-Archean Australian Shale (PAAS) in order to evaluate the nature and the chemistry of the water from which the carbonates precipitated (Taylor and McLennan, 1985; McLennan, 1989). Ce anomalies were calculated as $Ce/Ce^{*}= Ce/(0.5La+0.5Pr)$, and Pr anomalies as $Pr/Pr^{*}= Pr/(0.5Ce+0.5Nd)$, as per Bau and Dulski (1996). Carbonates, like BIF and some shales, tend to record the REE+Y signature of the ambient waters in which they formed. Their REE+Y pattern is specific to different aqueous environments:

- Modern seawater pattern characteristics are a positive La anomaly, a positive Gd anomaly, a positive Y anomaly, and LREE and MREE depletion relative to HREE (Kamber and Webb, 2001; Bolhar et al., 2004; Kamber et al., 2014). All of these characteristics are the result of different complexation behaviors of these elements in relation to organic ligands, pH, and [CO_3^{2-}] (Sholkovitz et al., 1994; Nozaki et al., 1997; Quinn et al., 2006). Moreover, a negative Ce anomaly is expressed when conditions are sufficiently oxidizing in the water column. All the characteristics listed above, with the exception of the positive Gd anomaly, are characteristics of modern deep sea venting fluids as well.

- An Archean seawater pattern revealed by multiple analyses of BIF data shows, in addition to modern seawater characteristics, a positive Eu anomaly due to the release of Eu by strong hydrothermal activity in the ocean at that time (Bolhar et al., 2004; Planavsky et al., 2010).
- Modern freshwaters (rivers and lakes) tend to have a uniform flat REE+Y pattern (Kamber et al., 2014). They can present Eu and Ce anomalies as a function of plagioclase weathering and pH.–Nevertheless, complications can arise when the catchment is principally composed of carbonate. In this case, rivers may take on a REE+Y pattern similar to seawater (Xu and Han, 2009).
- Waters from restricted ocean basins tend to record the La, Gd, and Y anomalies characteristic of open seawater, while the slope of the pattern may be reversed relative to normal seawater (HREE and MREE depletion relative to LREE) (Kamber et al., 2014).
- While the above relates to modern aqueous REE+Y features, as discussed above, there is strong evidence that many of these features extend back to the early Archean. One important exception is the Ce anomaly, which is generally absent in Archean chemical sediments (e.g., Bau and Dulski, 1996). While the residence time of Ce today is lower (0.05–0.13 ky for Ce) than its neighbors (e.g., 0.28 ky for Nd) (Alibo and Nozaki, 1999) due to oxidation of Ce(III) to less-soluble Ce(IV), in anoxic waters its residence time was likely closer to that of Nd before extensive Ce redox cycling, and in all scenarios, the short residence times for REE+Y in seawater makes them local rather than global proxies.

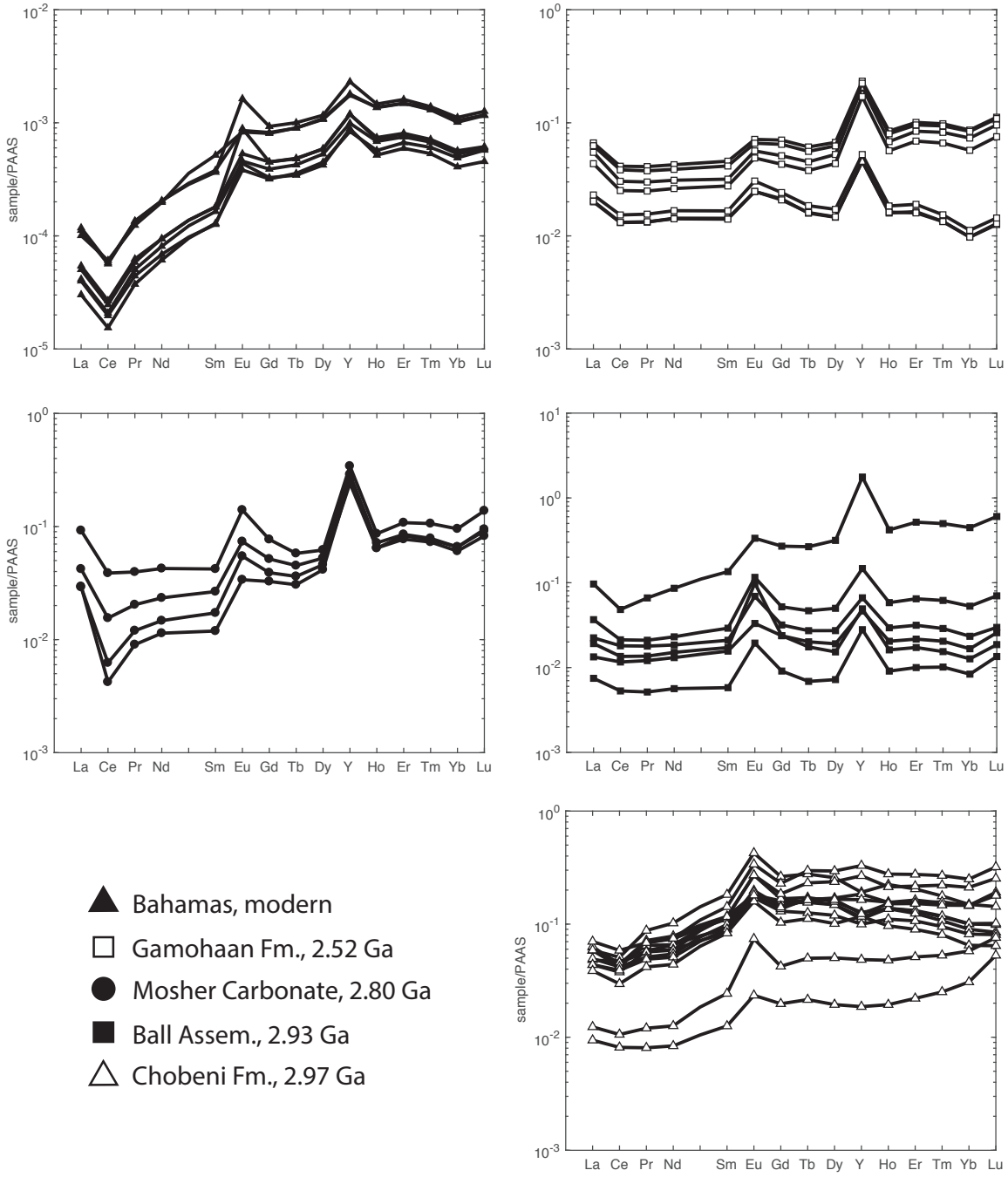

Figure DR3. Rare earth element and yttrium patterns of carbonate samples normalized to Post-Archean Australian Shale (PAAS; Taylor and McLennan, 1985; McLennan, 1989).

6. Evidence for marine origins of the studied carbonates

In order to attribute a seawater Mo signal to our carbonate samples and to compare them to marine shale data, their marine settings have to be established. Indeed, variability in carbonate deposition through geological time and among different environments is consequential. REE+Y patterns are a valuable proxy for constraining depositional environment, and accordingly, we attribute a marine setting to our samples if they record characteristics of Archean seawater REE+Y patterns as described previously:

- The modern Bahamas samples all have modern seawater characteristics with the exception of the Ce anomaly (c.f. Figure DR3). Indeed, a true negative Ce anomaly is lacking. We believe that this is a reflection of carbonate lithification in anoxic marine porewaters below the sediment-water interface (Visscher et al., 1998; Tostevin et al., 2016; see also sample description).
- The 2.52 Ga samples from the Gamohaan Fm. all record seawater characteristics (Figure DR3). Moreover, previous sedimentological study described the environment of the Gamohaan Formation as an open marine basin (Sumner et al., 1997); Altermann and Nelson, 1998) but also as including "vanished evaporites" (Gandin and Write, 2007). The absence of a Ce anomaly indicates a local absence of O_2 in the water column.
- The 2.80 Ga samples from the Mosher Carbonate record a global seawater REE+Y pattern with LREE and MREE depletion relative to HREE and positive La and Y anomalies (Figure DR3). Crystal fan and microbial samples indicate the presence of oxygen in the water column (negative Ce anomaly), while the stromatolite sample records anoxic conditions (no Ce anomaly), suggesting local redox variability. All samples display a positive Eu anomaly, typical of Archean seawater. The preservation

of an open seawater REE+Y signature suggests an open basin.

- The 2.93 Ga samples from Ball Assemblage all record seawater REE characteristics (Figure DR3). Recent studies suggest that deposition of the marine carbonate platform occurred during a volcanic hiatus (Sanborn-Barrie et al., 2001; McIntyre and Fralick., 2017). Positive Eu anomalies strongly indicate a connection to the open ocean. No samples analysed here from the 2.93 Ga Ball Assemblage display a true Ce anomaly, thus indicating local anoxia and anoxia in the area the where the REE concentrations in the water were derived.
- The 2.97 Ga samples from the Chobeni Fm. display a different REE+Y pattern than previous samples (Figure DR3). Indeed, no Y and La anomalies are present. Moreover, the slope is flat between MREE and HREE, which might signify proximity to the coast, similar to the 2.93 Ga samples from this study. Previous sedimentological and chemical studies described the Chobeni environment as an estuary or intertidal setting (i.e., Hicks et al., 2011; Siahi et al., 2016; 2018).

7. Potential contamination and post depositional effects on Mo isotopes in carbonates

Almost all samples with high SiO_2 concentrations (>50 wt%) showed no authigenic Mo enrichment and δ^{98}Mo that appear to trend to 0‰ with increasing degree of silicification (see Figure DR4b). Dolomitizing fluids are unlikely to have significantly affected the δ^{98}Mo ratios of the 2.80 Ga and 2.93 Ga samples, as no trend between the Mo isotopic composition and Mg is present (data not shown). A lack of correlation between Al_2O_3 and SiO_2 show that silicification rather than detrital contamination was the major determinant of SiO_2 content (Figure DR4c). The only contamination uncorrected on both Mo and δ^{98}Mo data comes from Fe (see Figure DR4a).

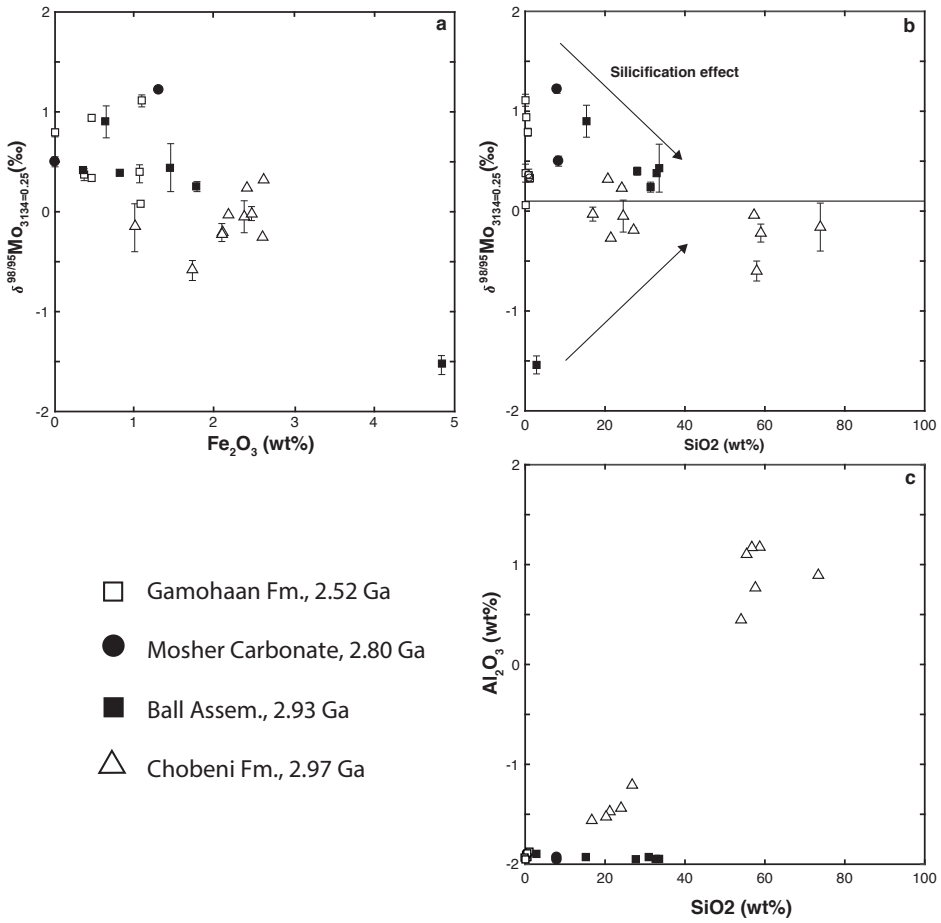

Figure DR4. Mo isotope compositions of carbonate samples from this study plotted as a function of (a) iron concentration and (b) silica concentration. For (b), data was corrected for detrital contamination and arrows indicate a putative silicification trend. (c) A lack of correlation between Al_2O_3 vs. SiO_2 demonstrates that the SiO_2 content in our Archean samples was determined largely by silicification as opposed to detrital contamination.

Ancient carbonate samples from this study have all been affected by diagenetic processes to some degree, as indicated by their light $\delta^{18}O$ values (Figure DR5b). The 2.93 Ga carbonates from the Ball Assemblage are characterized by a minimum $\delta^{18}O$ of -16.4‰, and may have been more strongly affected by diagenesis, especially dolomitized samples in which Sr isotope compositions appear to have been be reset (McIntyre and Fralick, 2017). The extent to which the $\delta^{98}Mo$ composition of these samples has been affected remains unclear, but this is

critical for assessing the reliability of the δ^{98}Mo signal with respect to Neoarchean seawater.

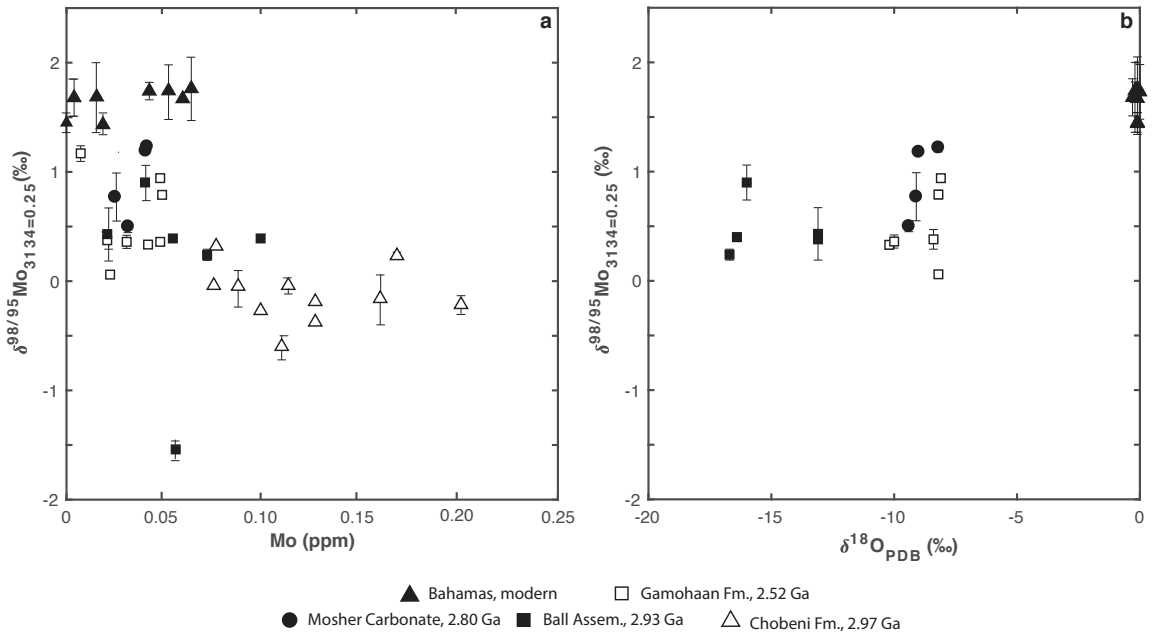

Figure DR5. Mo isotope compositions of carbonate samples from this study plotted as a function of (a) Mo concentration determined by isotope dilution and (b) oxygen isotope composition of carbonates.

The possibility of diagenetic alteration or resetting of the δ^{98}Mo ratio in carbonates has been addressed previously (Romaniello et al., 2016; Eroglu et al., 2015; Voegelin et al., 2009). Romaniello et al. (2016) studied modern carbonates from the Bahamas and observed a close relationship between the δ^{98}Mo of modern samples and the H_2S_{aq} concentration in sediment pore waters. Organic-rich carbonates typically display significant H_2S_{aq} concentrations in pore waters, and correspondingly, high carbonate bound Mo concentrations, consistent with the redox sensitive nature of Mo. Conversely, organic-lean white carbonates are generally characterized by low Mo concentrations attended by low H_2S_{aq} in pore waters. Thus, carbonates with high pore water H_2S_{aq} concentrations tend to quantitatively capture the global seawater δ^{98}Mo ratio, while carbonates with lower H_2S_{aq} levels record lighter δ^{98}Mo values

that do not fully capture the global seawater signal, but a lower value. In other words, more strongly-reducing conditions during early diagenesis lead to carbonates with higher Mo concentrations and a heavier δ^{98}Mo isotopic ratio that is likely to be more representative of the global δ^{98}Mo seawater value. In older carbonates, however, the relationship between δ^{98}Mo and Mo concentration that is observed from modern carbonates is either non-existent (Wen et al., 2011; Eroglu et al., 2015; Voegelin et al., 2010), or if present, inverse to that of modern samples (Voegelin et al., 2010). Previous studies agree that carbonate diagenesis drives δ^{98}Mo to lighter values. Given that initial $\delta^{98}Mo_{Carb} = \delta^{98}Mo_{SW}$, and that bacteria preferentially uptake lighter Mo isotopes (Zerkle et al., 2011), microbial sulfur cycling that occurs in the reducing pore waters found in stromatolites should lead to a post-depositional signal of $\delta^{98}Mo_{Carb} < \delta^{98}Mo_{SW}$ (Eroglu et al., 2015). Additionally, the absorption of Mo on Fe-(hydro)oxides surfaces in suboxic pore water should similarly produce a signal where $\delta^{98}Mo_{Carb} < \delta^{98}Mo_{SW}$ (Goldberg et al. 2009; Voegelin et al., 2009). McManus et al. (2002) similarly proposed that the diagenesis of authigenic carbonate-hosted Mo leads to light isotope enrichment in the sediment. Indeed, even organic-rich, suboxic sapropels have been shown to have δ^{98}Mo values lighter than expected due to diagenetic effects (Reizt et al., 2007). Here, contrary to Romaniello et al. (2016), our global data display an inverse trend between δ^{98}Mo ratios and Mo concentrations (Figure DR5a). This mirrors the findings of Voegelin et al. (2010), who observed a similar relationship in the GKP01 core that samples the 2.64-2.50 Ga Ghaap Group, South Africa, and records $\delta^{18}O_{PDB} < -10‰$ as well (Fisher et al., 2009).

Finally, while organic matter preferentially sequesters light Mo isotopes (King et al., 2018), we calculate that at Mo concentrations typical for Neoarchean and older shales, this process was unlikely to have affected the dissolved Mo reservoir of open seawater. Quite simply, taking the average concentration of ~1 ppm Mo for Neoarchean and older shales (Figure 1C),

if one attributes a concentration of 1 ppm Mo to the totality of carbon buried annually today (10^{13} mol C / year), this represents only 0.0007% of the modern Mo exit flux (or 0.75% if we conservatively assume a Neoarchean exit flux 1/1000 smaller than today; see Table DR7). Therefore, it appears highly unlikely that the association of light Mo with organic matter in the Neoarchean had much of a role, if any, in the heavy isotopic enrichment of seawater Mo at that time.

References cited

Addison, W. D., Brumpton, G. R., Vallini, D. A., McNaughton, N. J., Davis, D. W., Kissin, S. A., Fralick, P. W., and Hammond, A. L., 2005, Discovery of distal ejecta from the 1850 Ma Sudbury impact event: Geology, v.33, p. 193–196, doi: 10.1130/G21048.1.

Alibo, D. S., and Nozaki, Y., 1999, Rare earth elements in seawater: Particle association, shale- normalization, and Ce oxidation: Geochimica et Cosmochimica Acta, v. 63, p. 363–372.

Altermann, W., and Nelson, D. R., 1998, Sedimentation rates, basin analysis and regional correlations of three Neoarchaean and Palaeoproterozoic sub-basins of the Kaapvaal craton as inferred from precise U–Pb zircon ages from volcaniclastic sediments: Sedimentary Geology, v. 120, p. 225-256, doi: 10.1016/S0037-0738(98)00034-7.

Arnold, G. L., Anbar, A., Barling, J., and Lyons, T., 2004, Molybdenum isotope evidence for widespread anoxia in mid-Proterozoic oceans: Science, v. 304, p. 87–90, doi: 10.1126/science.1091785.

Asael, D., Tissot, F. L., Reinhard, C. T., Rouxel, O., Dauphas, N., Lyons, T. W., Ponzevera, E., Liorzou, C., and Chéron, S., 2013, Coupled molybdenum, iron and uranium stable isotopes as oceanic paleoredox proxies during the Paleoproterozoic Shunga Event: Chemical Geology, v. 362, p. 193–210, doi: 10.1016/j.chemgeo.2013.08.003.

Barling, J., Arnold, G. L., and Anbar, A., 2001, Natural mass-dependent variations in the isoto- pic composition of molybdenum: Earth and Planetary Science Letters, v.193, p. 447–457, doi: 10.1016/S0012-821X(01)00514-3.

Bau, M., and Dulski, P., 1996, Distribution of yttrium and rare-earth elements in the Penge and Kuruman iron-formations, Transvaal Supergroup, South Africa: Precambrian Research, v. 79, p. 37–55.

Beukes, N. J., and Lowe, D. R., 1989, Environmental control on diverse stromatolite morphologies in the 3000 Myr Pongola Supergroup, South Africa: Sedimentology v. 36, p. 383–397.

Blake, T. S., 1993, Late Archaean crustal extension, sedimentary basin formation, flood basalt volcanism and continental rifting: the Nullagine and Mount Jope Supersequences, Western Australia: Precambrian Research, v. 60, p. 185–241.

Bolhar, R., Kamber, B. S., Moorbath, S., Fedo, C. M., and Whitehouse, M. J., 2004, Characterisation of early Archaean chemical sediments by trace element signatures: Earth and Planetary Science Letters v. 222, p. 43–60, doi: 10.1016/j.epsl.2004.02.016.

Collier, R. W., 1985, Molybdenum in the Northeast Pacific Ocean 1: Limnology and Oceanography, v. 30, p. 1351-1354.

Corfu, F., and Wallace, H., 1986, U–Pb zircon ages for magmatism in the Red Lake greenstone belt, northwestern Ontario: Canadian Journal of Earth Sciences v. 23, p.27–42.

Corfu, F., and Stone, D., 1998, The significance of titanite and apatite U-Pb ages: constraints for the post-magmatic thermal-hydrothermal evolution of a batholithic complex, Berens River area, northwestern Superior Province, Canada: Geochimica et Cosmochimica Acta v. 62, p. 2979–2995.

Edgcomb, V. P., Bernhard, J. M., Summons, R. E., Orsi, W., Beaudoin, D., and Visscher, P. T., 2014, Active eukaryotes in microbialites from Highborne Cay, Bahamas, and Hamelin Pool (Shark Bay), Australia: The ISME journal v. 8, 418, doi: 10.1038/ismej.2013.130.

Emerson, S. R., and Huested, S. S., 1991, Ocean anoxia and the concentrations of molybdenum and vanadium in seawater: Marine Chemistry, v. 34, p. 177-196.

Eroglu, S., Schoenberg, R., Wille, M., Beukes, N., and Taubald, H., 2015, Geochemical stratigraphy, sedimentology, and Mo isotope systematics of the ca. 2.58–2.50 Ga-old Transvaal Supergroup carbonate platform, South Africa: Precambrian Research, v. 266, p. 27–46, doi: 10.1016/j.precamres.2015.04.014.

Fischer, W., Schroeder, S., Lacassie, J., Beukes, N., Goldberg, T., Strauss, H., Horstmann, U., Schrag, D., and Knoll, A., 2009, Isotopic constraints on the Late Archean carbon cycle from the Transvaal Supergroup along the western margin of the Kaapvaal Craton, South Africa: Precambrian Research v. 169, p. 15–27.

Fralick, P.W., Hollings, P. and King, D., 2008, Stratigraphy, geochemistry and depositional environments of Mesoarchean sedimentary units in western Superior Province: implications for generation of early crust. In, K.C. Kondie, V. Pease (Eds.), When did Plate Tectonics begin on Planet Earth? Geological Society of America, Special Paper 440, p. 77-96. , doi: 10.1130/2008.2440(04).

Fralick, P.W., and Riding, R., 2015, Steep Rock Lake: Sedimentology and geochemistry of an Archean carbonate platform: Earth Science Reviews, v. 151, p. 132-175, doi:10.1016/j.earscirev.2015.10.006

Gandin, A. and Wright, D.T. 2007, Evidence of vanished evaporites in the Neoarchean carbonates of South Africa: In Schreiber, B.C., Lugli, S. and Babel, M (Eds.): Evaporites through space and time. Geol. Soc. London, Spec. Publ. 285, 285-308.

Goldberg, T., Archer, C., Vance, D., and Poulton, S. W., 2009, Mo isotope fractionation during adsorption to Fe (oxyhydr) oxides: Geochimica et Cosmochimica Acta v. 73, p. 6502–6516.

Goldberg, T., Gordon, G., Izon, G., Archer, C., Pearce, C. R., McManus, J., and Anbar, A. D., Rehkämper, M., 2013, Resolution of inter-laboratory discrepancies in Mo isotope data:

an intercalibration: Journal of Analytical Atomic Spectrometry, v. 28, p. 724–735, doi: 10.1039/c3ja30375f.

Greber, N. D., Siebert, C., Nägler, T. F., and Pettke, T., 2012, $\delta^{98/95}$Mo values and molybdenum concentration data for NIST SRM 610, 612 and 3134: Towards a common protocol for reporting Mo data: Geostandards and Geoanalytical Research, v. 36, p. 291–300, doi: 10.1111/j.1751-908X.2012.00160.x.

Gruau, G., Dia, A., Olivie-Lauquet, G., Davranche, M., and Pimay, G., 2004, Controls on the distribution of rare earth elements in shallow groundwater. Water Research, v. 38, p. 3576-3586.

Hicks, N., Dunlevey, J., and Liu, K., 2011, A new stromatolite occurrence in the Nsuze Group, Pongola Supergroup of northern KwaZulu-Natal, South Africa: South African Journal of Geology v. 114, p. 195–200, doi: 10.2113/gssajg.114.2.195.

Holland, H. D., 1978, The chemistry of the atmosphere and oceans, v. 1.

Holland, H. D., 2002, Volcanic gases, black smokers, and the Great Oxidation Event: Geochimica et Cosmochimica Acta, v. 66, p. 3811-3826, doi: 10.1016/S0016-7037(02)00950-X.

Kamber, B. S., and Webb, G. E., 2001, The geochemistry of late Archaean microbial carbonate: implications for ocean chemistry and continental erosion history: Geochimica et Cosmochimica Acta v. 65, p. 2509–2525, doi: 10.1016/S0016-7037(01)00613-5.

Kamber, B. S., Webb, G. E., and Gallagher, M., 2014, The rare earth element signal in Archaean microbial carbonate: information on ocean redox and biogenicity: Journal of the Geological Society, v.171, p.745-763, doi: 10.1144/jgs2013-110.

King, E. K., Perakis, S. S., and Pett-Ridge, J. C., 2018, Molybdenum isotope fractionation during adsorption to organic matter: Geochimica et Cosmochimica Acta, v. 222, p. 584–598, doi: 10.1016/j.gca.2017.11.014.

Lalonde, S. V., and Konhauser, K. O., 2015, Benthic perspective on Earth's oldest evidence for oxygenic photosynthesis: Proceeding of the National Academy of Sciences, v. 112, p. 995)1000, doi: 0.1073/pnas.1415718112.

McIntyre, T., and Fralick, P., 2017, Sedimentology and Geochemistry of the 2930 Ma Red Lake– Wallace Lake Carbonate Platform, Western Superior Province, Canada: The Depositional Record v. 3, p. 258–287, doi: 10.1002/dep2.36.

McLennan, S., 1989, Geochemistry and mineralogy of rare earth elements: Reviews in Mineralogy v. 21, p. 169–200.

McManus, J., Nägler, T. F., Siebert, C., Wheat, C. G., and Hammond, D. E., 2002, Oceanic molybdenum isotope fractionation: Diagenesis and hydrothermal ridge-flank alteration: Geochemistry, Geophysics, Geosystems v. 3, p. 1–9, doi: 10.1029/2002GC000356.

Mukasa, S. B., Wilson, A. H., and Young, K. R., 2013, Geochronological constraints on the magmatic and tectonic development of the Pongola Supergroup (Central Region), South Africa: Precambrian Research v. 224, p. 268–286, doi: 10.1016/j.precamres.2012.09.015.

Myshrall, K., Mobberley, J., Green, S., Visscher, P., Havemann, S., Reid, R., and Foster, J., 2010, Biogeochemical cycling and microbial diversity in the thrombolitic microbialites of Highborne Cay, Bahamas: Geobiology v. 8, p. 337–354, doi: 0.1111/j.1472-4669.2010.00245.x.

Nägler, T. F., Anbar, A. D., Archer, C., Goldberg, T., Gordon, G. W., Greber, N. D., Siebert, C., Sohrin, Y., and Vance, D., 2014, Proposal for an international molybdenum isotope measurement standard and data representation: Geostandards and Geoanalytical Research, v. 38, p. 149–151, doi: 10.1111/j.1751-908X.2013.00275.x.

Neubert, N., Nägler, T. F., and Böttcher, M. E., 2008, Sulfidity controls molybdenum isotope fractionation into euxinic sediments: Evidence from the modern black sea: Geology v. 36, p. 775–778, doi: 10.1130/G24959A.1.

Nozaki, Y., Zhang, J., and Amakawa, H., 1997, The fractionation between Y and Ho in the marine environment: Earth and Planetary Science Letters v. 148, p. 329–340.

Planavsky, N., Bekker, A., Rouxel, O. J., Kamber, B., Hofmann, A., Knudsen, A., and Lyons, T. W., 2010, Rare earth element and yttrium compositions of Archean and Paleoproterozoic Fe formations revisited: new perspectives on the significance and mechanisms of deposition: Geochimica et Cosmochimica Acta v. 74, p. 6387–6405.

Poulson, R. L., Siebert, C., McManus, J., and Berelson, W. M., 2006, Authigenic molybdenum isotope signatures in marine sediments: Geology, v. 34, p. 617–620, doi: 10.1130/G22485.1.

Quinn, K. A., Byrne, R. H., and Schijf, J., 2006., Sorption of yttrium and rare earth elements by amorphous ferric hydroxide: influence of solution complexation with carbonate: Geochimica et Cosmochimica Acta v. 70, p. 4151–4165, doi: 10.1016/j.gca.2006.06.014.

Reitz, A., Wille, M., Nägler, T. F., and de Lange, G. J., 2007, Atypical Mo isotope signatures in eastern Mediterranean sediments: Chemical Geology v. 245, p. 1–8, doi: 10.1016/j.chemgeo.2007.06.018.

Riding, R., Fralick, P., and Liang, L., 2014, Identification of an Archean marine oxygen oasis: Precambrian Research v. 251, p. 232–237, doi: 10.1016/j.precamres.2014.06.017.

Romaniello, S. J., Herrmann, A. D., and Anbar, A. D., 2016, Syndepositional diagenetic control of molybdenum isotope variations in carbonate sediments from the Bahamas: Chemical Geology v. 438, p. 84–90, doi: 10.1016/j.chemgeo.2016.05.019.

Rongemaille, E., Bayon, G., Pierre, C., Bollinger, C., Chu, N., Fouquet, Y., Riboulot, V., and Voisset, M., 2011, Rare earth elements in cold seep carbonates from the Niger delta: Chemical Geology v. 286, p. 196–206, doi: 10.1016/j.chemgeo.2011.05.001.

Sanborn-Barrie, M., Parker, J., and Skulski, T., 2001, Three hundred million years of tectonic history recorded by the Red Lake greenstone belt, Ontario: Natural Resources Canada, Geological Survey of Canada.

Sholkovitz, E. R., Landing, W. M., and Lewis, B. L., 1994, Ocean particle chemistry: the fractionation of rare earth elements between suspended particles and seawater: Geochimica et Cosmochimica Acta v. 58, p. 1567–1579.

Siahi, M., Hofmann, A., Hegner, E., and Master, S., 2016, Sedimentology and facies analysis of Mesoarchaean stromatolitic carbonate rocks of the Pongola Supergroup, South Africa: Precambrian Research v. 278, p. 244–264, doi: 10.1016/j.precamres.2016.03.004.

Siahi, M., Hofmann, A., Master, S., Wilson, A., and Mayr, C., 2018, Trace element and stable (C, O) and radiogenic (Sr) isotope geochemistry of stromatolitic carbonate rocks of the Mesoar- chaean Pongola Supergroup: Implications for seawater composition: Chemical Geology v. 476, p. 389–406, doi: 10.1016/j.chemgeo.2017.11.036.

Siebert, C., Nägler, T. F., and Kramers, J. D., 2001, Determination of molybdenum isotope fractionation by double-spike multicollector inductively coupled plasma mass spectrometry: Geochemistry, Geophysics, Geosystems v. 2.

Siebert, C., Nägler, T. F., von Blanckenburg, F., and Kramers, J. D., 2003, Molybdenum isotope records as a potential new proxy for paleoceanography: Earth and Planetary Science Letters v. 211, p. 159–171, doi: 10.1016/S0012-821X(03)00189-4.

Siebert, C., McManus, J., Bice, A., Poulson, R., and Berelson, W. M., 2006, Molybdenum isotope signatures in continental margin marine sediments: Earth and Planetary Science Letters, v. 241, p. 723–733, doi: 10.1016/j.epsl.2005.11.010.

Sumner, D. Y., 1997, Carbonate precipitation and oxygen stratification in late Archean seawater as deduced from facies and stratigraphy of the Gamohaan and Frisco

formations, Transvaal Supergroup, South Africa: American Journal of Science v. 297, p. 455–487.

Sumner, D. Y., and Bowring, S. A., 1996, U - Pb geochronologic constraints on deposition of the Campbellrand Subgroup, Transvaal Supergroup, South Africa: Precambrian Research v. 79, p. 25–35.

Sumner, D. Y., and Grotzinger, J. P., 2004, Implications for Neoarchaean ocean chemistry from primary carbonate mineralogy of the Campbellrand-Malmani platform, South Africa: Sedimentology v. 51, p. 1273–1299, doi: 10.1111/j.1365-3091.2004.00670.x.

Taylor, S. R., and McLennan, S. M., 1985, The continental crust: its composition and evolution, an examination of the geochemical record preserved in sedimentary rocks: Blackwell Scientific, Oxford, 312 p.

Thorne, A., and Trendall, A. F., 2001, Geology of the Fortescue Group, Pilbara Craton, Western Australia: Geological Survey, Bulletin 144, 249 p.

Tomlinson, K. Y., Davis, D. W., Stone, D., and Hart, T. R., 2003, U–Pb age and Nd isotopic evidence for Archean terrane development and crustal recycling in the south-central Wabi- goon subprovince, Canada: Contributions to Mineralogy and Petrology v. 144, p. 684–702, doi: 10.1007/s00410-002-0423-0.

Tostevin, R., Shields, G. A., Tarbuck, G. M., He, T., Clarkson, M. O., and Wood, R. A., 2016, Effective use of cerium anomalies as a redox proxy in carbonate-dominated marine settings: Chemical Geology, v. 438, p. 146-162, doi: 10.1016/j.chemgeo.2016.06.027.

Veizer, J., Compston, W., Hoefs, J., and Nielsen, H., 1982, Mantle buffering of the early oceans: Naturwissenschaften v. 69, p. 173–180.

Visscher, P. T., Reid, R. P., Bebout, B. M., Hoeft, S. E., Macintyre, I. G., and Thompson, J. A., 1998, Formation of lithified micritic laminae in modern marine stromatolites (bahamas): the role of sulfur cycling: American Mineralogist, v. 83, p. 1482–1493.

Voegelin, A. R., Nägler, T. F., Samankassou, E., and Villa, I. M., 2009, Molybdenum isotopic composition of modern and carboniferous carbonates: Chemical Geology v. 265, p. 488–498, doi: 10.1016/j.chemgeo.2009.05.015.

Voegelin, A. R., Naägler, T. F., Beukes, N. J., and Lacassie, J. P., 2010, Molybdenum isotopes in late Archean carbonate rocks: implications for Early earth oxygenation: Precambrian Research v. 182, p. 70–82, doi: 10.1016/j.precamres.2010.07.001.

Wen, H., Carignan, J., Zhang, Y., Fan, H., Cloquet, C., and Liu, S., 2011, Molybdenum isotopic records across the Precambrian-Cambrian boundary: Geology v. 39, p. 775–778, doi: 10.1130/G32055.1.

Wilks, M., and Nisbet, E., 1985, Archaean stromatolites from the Steep Rock Group, northwestern Ontario, Canada: Canadian Journal of Earth Sciences v. 22, p. 792–799.

Wille, M., Nebel, O., Van Kranendonk, M. J., Schoenberg, R., Kleinhanns, I. C., and Ellwood, M. J., 2013, Mo–Cr isotope evidence for a reducing Archean atmosphere in 3.46–2.76 Ga black shales from the Pilbara, Western Australia: Chemical Geology, v. 340, p. 68–76, doi: 10.1016/j.chemgeo.2012.12.018.

Xu, Z., and Han, G., 2009, Rare earth elements (REE) of dissolved and suspended loads in the Xijiang River, South China: Applied Geochemistry v. 24, p.1803–1816, doi: 10.1016/j.apgeochem.2009.06.001.

Zerkle, A., Scheiderich, K., Maresca, J., Liermann, L., and Brantley, S., 2011, Molybdenum isotope fractionation by cyanobacterial assimilation during nitrate utilization and N_2 fixation: Geobiology v. 9, p. 94–106, doi: 10.1111/j.1472-4669.2010.00262.x.